A Journal of the Gesellschaft Deutscher Chemiker

Angewandte International Edition GDCh Chemie

www.angewandte.org

Accepted Article

Title: Synergic Interplay Between Halogen Bond and Hydrogen Bond in the Activation of a Neutral Substrate in a Nanoconfined Space

Authors: Carmine Gaeta, Pellegrino La Manna, Margherita De Rosa, Carmen Talotta, Antonio Rescifina, Giuseppe Floresta, Annunziata Soriente, and Placido Neri

To be cited as: *Angew. Chem. Int. Ed.* 10.1002/anie.201909865
Angew. Chem. 10.1002/ange.201909865

Link to VoR: http://dx.doi.org/10.1002/anie.201909865
http://dx.doi.org/10.1002/ange.201909865

WILEY-VCH

10.1002/anie.201909865

WILEY-VCH

RESEARCH ARTICLE

Synergic Interplay Between Halogen Bond and Hydrogen Bond in the Activation of a Neutral Substrate in a Nanoconfined Space

Pellegrino La Manna, Margherita De Rosa, Carmen Talotta,* Antonio Rescifina,* Giuseppe Floresta, Annunziata Soriente, Carmine Gaeta,* Placido Neri

Dedication ((optional))

Abstract: *The principle of the "amplified halogen bonding (XB) in a small space" is here exploited as a catalytic tool for the activation of an XB acceptor substrate in a nanoconfined environment. The inner cavity of the resorcinarene capsule has been equipped with an XB catalyst bearing an ammonium unit acting as a Trojan horse to drive the catalyst inside the capsule. In the presence of the XB catalyst **5**, the capsule is able to catalyze a Michael reaction between N-methylpyrrole and methyl vinyl ketone. In the bulk medium, in the absence of the resorcinarene capsule, the XB catalyst **5** was catalytically ineffective. Quantum-mechanical investigations highlighted that the Michael reaction proceeds through the activation of the carbonyl by synergistically enhanced halogen/hydrogen bonding interactions, and takes place in an open pentameric capsule.*

Introduction

The halogen bonding (XB)[1] interaction is considered as an useful tool in supramolecular chemistry[2] for engineering new materials[3] and for the self-assembly of supramolecules and interpenetrated architectures.[2,3] XB is a secondary interaction between a covalently bound halogen atom in a R–X compound (the "*XB donor*", where X = I, Br, Cl, F, and R = C or any other atom including even I, for example) and a Lewis base (the "*XB acceptor*").[4] This interaction is highly directional, and its strength strictly depends on the structures of the XB donor and acceptor partners.[4] Thus, the presence of electron-withdrawing groups in R, which are able to polarize the X atom, increases its XB donor ability and consequently the strength of XB interaction.

Recently, an increasing attention has been devoted to exploiting the XB interaction in solution, where the polarity of the medium has a crucial role. In this regard, the potential application of XB donor derivatives in organocatalysis,[5,6] is attracting more interest in the scientific community. Thus, for example, the XB interaction has been exploited for the activation of carbonyl compounds,[7] activation of substrates by halides abstraction,[8] and activation of neutral substrates.[9]

In the last decades, many efforts have been devoted to the study of reactions catalyzed in nanoconfined spaces.[10] Cram [11] and Rebek[12] earlier showed that when the molecules are confined inside a capsule, their chemical behavior can diverge from the usual one observed in the bulk medium. When the substrates are confined in the restricted space inside a molecular capsule, the proximity effect between them, and their hyper concentration due to the nano-confinement, induce a reaction rate acceleration, thus mimicking the *modus operandi* of natural enzymes.[10] The most impressive aspect of the catalysis in nanoconfined spaces is that the reactivity of the molecules can be smartly driven to disobey classical behavior.[13] Recently, in an elegant work by Fujita, Metrangolo, and Resnati,[3b] the authors highlighted that the confined space inside a self-assembled cage enhances the halogen bonding between XB donors and XB acceptors. Previously, Rebek[3c] also showed that the encapsulation of both XB partners into the nanoconfined space of a dimeric capsule *amplified the halogen bonding interaction* and allowed its NMR characterization.

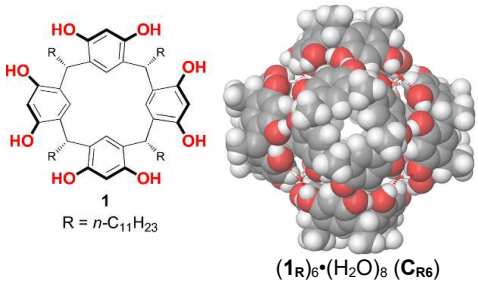

Figure 1. Chemical drawing of *C*-undecylresorcin[4]arene **1** (left) and a reduced model (R = Me) of the hexameric capsule $(\mathbf{1_R})_6$•$(H_2O)_8$ ($\mathbf{C_{R6}}$) (right).

On these bases, we have envisioned that the "*halogen bonding amplification in a small space*", can be exploited as a tool for XB catalysis inside a self-assembled resorcinarene capsule. The hexameric capsule $(\mathbf{1})_6$•$8H_2O$ ($\mathbf{C_6}$), originally reported by Atwood,[14] is obtained by self-assembly of six resorcinarene **1** units and eight water molecules (Figure 1), and has been largely exploited as nanoreactor[10a,c,e,f,j,k] thanks to its capacity to host selectively the substrates and to accelerate the organic reactions with excellent chemo-, regio-, and stereoselectivity. The advantage of using such nanocontainers as a catalyst, with respect to smaller macrocycles, is that the larger cavity can be easily engineered, for example, by introducing specific artificial

Dr. P. La Manna, Dr. C. Talotta, Dr. M. De Rosa, Prof. Dr. A. Soriente, Prof. Dr. C. Gaeta, Prof. Dr. P. Neri
Laboratory of Supramolecular Chemistry,
Dipartimento di Chimica e Biologia "A. Zambelli"
Università di Salerno
Via Giovanni Paolo II, 132, I-84084, Fisciano (Salerno), Italy
E-mail: cgaeta@unisa.it; ctalotta@unisa.it

Dr. G. Floresta, Prof. A. Rescifina,
Dipartimento di Scienze del Farmaco, Università di Catania, viale Andrea Doria, 6, 95125 Catania, Italy.
E-mail: arescifina@unict.it

Supporting information for this article is given via a link at the end of the document.

10.1002/anie.201909865

cofactors.[15] Commonly, the π-electron-rich cavity of **C6** shows a high affinity for cationic ammonium groups,[10] which can be considered as an ideal recognition motif useful to drive the molecular encapsulation of appropriate guests inside the hexameric capsule. Based on these considerations, we here report the first example of a halogen bonding catalysis in a nanoconfined environment synergistically enhanced by hydrogen bonding interactions. In particular, we have focused our attention on the Michael reaction reported in Scheme 1, employing *p*-iodophenyltrimethyl-ammonium salts **5** as XB-catalysts. Our design is prompted by the idea that the trimethylammonium group is able to establish cation···π interactions with the electron-rich aromatic cavity of **C6**, while the *p*-iodophenyl moiety is the active XB donor. In addition, the Me_3N^+ moiety could act as an electron-withdrawing group able to polarize the I atom, thus increasing its XB donor ability.

Results and Discussion

Initially, we investigated the reaction between *N*-methylpyrrole **2** and methyl vinyl ketone **3** in the presence of resorcinarene **1** (Scheme 1), in water-saturated $CDCl_3$ as the solvent, in order to form the **C6** capsule. When the reaction mixture (Table 1, entry 3) was stirred at 50 °C for 16 h, the product **4** was obtained in 12% yield, whereas no product was obtained in the absence of **1** (entry 4). Interestingly, when *p*-iodophenyltrimethylammonium iodide **5a** was added to the mixture of **1**, **2**, and **3** in water-saturated $CDCl_3$, a 98% yield of product **4** was obtained after 16 h at 50 °C (Table 1, entry 2). These results confirm the crucial role played by the *p*-iodophenyltrimethylammonium iodide in the catalysis of the Michael reaction reported in Scheme 1.
Now, the question arises whether the resorcinarene capsule plays still a catalytic role in the presence of **5a**.

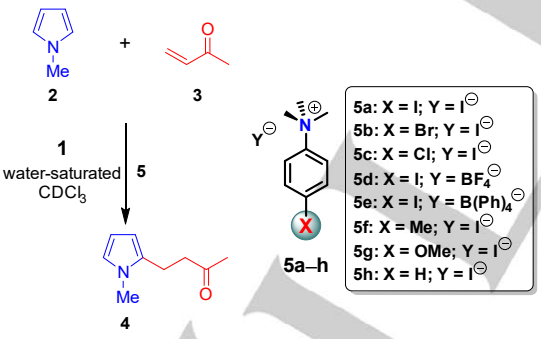

Scheme 1. Halogen bonding catalyzed Michael reaction between *N*-methylpyrrole **2** and methyl vinyl ketone **3** in the presence of **1**.

In addition to what noted in entry 4, when the reaction in Scheme 1 was performed in the presence of the non-halogenated phenyltrimethylammonium **5h** (Table 1, entry 18) a significant decrease in yield was obtained (−65%), respect to the best performing reaction. This result highlights the crucial role played by the halogen-bond in the activation of substrate **3** (vide infra). Summarizing, these preliminary results indicate that the simultaneous presence of both **1** and *p*-iodophenyltrimethylammonium iodide **5a** is crucial for the catalysis of the Michael reaction (Scheme 1) between **2** and **3**. Also, these data strongly indicate that the reaction reported in Scheme 1 occurs in the nanoconfined space inside a resorcinarene capsule through an XB activation of the substrate **3**, which is ineffective in the bulk medium in the absence of **1**.

Table 1. Halogen bonding catalyzed Michael reaction between *N*-methylpyrrole **2** and methylvinylketone **3** in the presence of **1**.

Entry[a]	T (°C)	Halogen bonding catalyst (20%)	Capsule amount (mol%)	Yield of **4** (%)[b]
1	30	**5a**	26	82
2	50	**5a**	26	98
3	50	—	26	12
4	50	**5a**	—	—
5[c]	50	**5a**	26	88
6[d]	50	**5a**	26	1
7[e]	50	**5a**	26	—
8	50	**5b**	26	45
9	50	**5b**	—	—
10	50	**5c**	26	53
11	50	**5c**	—	—
12	50	**5d**	26	5
13	50	**5d**	—	—
14	50	**5e**	26	50
15	50	**5e**	—	—
16	50	**5f**	26	24[f]
17	50	**5g**	26	8[g]
18	50	**5h**	26	33

[a] Reaction conditions: **2** (0.59 M), **3** (0.15 M), **1** (0.0063 M) in 1.1 mL of water-saturated $CDCl_3$, 16 h. [b] Isolated yield. [c] Reaction time: 4 h. [d] The reaction was performed in the presence of hexamethonium bromide (0.76 M). [e] The reaction was carried out in the presence of DMSO. [f,g] The 25%[f] and 18%[g] of 2,5-disubstituted product was obtained.

This was confirmed by the finding that, when the reaction in Scheme 1 was performed in the presence of hexamethonium bromide, a known competitive guest,[16] only traces (1%) of **4** were detected after 16 h at 50 °C (Table 1, entry 6). Under these conditions, the hexamethonium bromide occupying the cavity of capsule **C6** acts as an inhibitor lowering the yield. In addition, the ^{1}H NMR spectrum of the reaction mixture in the presence of hexamethonium bromide featured shielded signals at negative chemical shifts values attributable to the cation inside the cavity of **C6**. Furthermore, product **4** was not observed when the reaction reported in Scheme 1 was performed in the presence of solvents that compete for hydrogen bonding (*e.g.*, DMSO, Table 1, entry 7).
Following a standard protocol previously reported,[13,15] evidences for the encapsulation of the reagents and co-catalyst **5a** inside the **C6** capsule were provided by 1D and 2D-NMR studies (see the Supporting Information). Moreover, when methyl vinyl ketone **3**

was added to a water-saturated $CDCl_3$ solution of **C_6**, the ^{1}H NMR spectrum (see the Supporting Information) of the mixture showed the presence of signals in the upfield region, at negative values, indicative of the presence of **3** inside **C_6**. Regarding the encapsulation of **5a**, the ^{1}H NMR spectrum of the **5a**/**C_6** mixture in water-saturated $CDCl_3$ evidenced the presence of a signal at 1.32 ppm which correlates, in the HSQC spectrum, with a carbon resonance at 55.2 ppm attributable to the methyls of the $^+N(Me)_3$ group of **5a**.

The shielding of the $^+N(Me)_3$ signal in the high-field region of the ^{1}H NMR spectrum by 3.78 ppm ($\Delta\delta = \delta_{free} - \delta_{complexed} = 4.00 - 1.32$) is strongly indicative of the inclusion of **5a** inside the aromatic cavity of **C_6**. Analogously, the aromatic hydrogen atoms of **5a** experienced a complexation induced shift (CIS) of 0.42 ($\Delta\delta = \delta_{free} - \delta_{complexed} = 7.86 - 7.24$) and 1.52 ppm ($\Delta\delta = \delta_{free} - \delta_{complexed} = 7.62 - 6.10$).

In conclusion, it is clear that *p*-iodophenyltrimethylammonium XB-catalyst **5a** is enclosed inside the cavity of **C_6** driven by cation$\cdots\pi$ interactions (Scheme 2) and 1D and 2D-NMR studies highlighted that also the reactants **2** and **3** are confined inside the hexameric capsule **C_6**.

To corroborate the catalytic role of this halogen bonding interaction, we studied the reaction reported in Scheme 1 using *p*-X-phenyltrimethylammonium salts **5b**–**d** (Table 1, entries 8, 10, and 12). As it is well established,[1,4] the XB strength increase with the polarizability of the XB donor atom, that is, F < Cl < Br < I. Accordingly, when *N*-methylpyrrole **2** was reacted with **3**, in the presence of **1**, and *p*-bromophenyltrimethylammonium iodide **5b,** then product **4** was obtained in 45% yield (Table 1, entry 8), while a 53% of **4** was obtained using *p*-chlorophenyltrimethylammonium iodide **5c** (Table 1, entry 10). In addition, in these cases, the XB catalysts **5b** and **5c** do not work in the bulk medium, in the absence of capsule (Table 1, entries 9 and 11).

With these results in hand, we investigated the role of the counteranion of the trimethylammonium cation on the efficiency of the catalytic system. When the BF_4^- salt of *p*-iodophenyltrimethylammonium (**5d**) was mixed with **1**, **2**, and **3**, in water-saturated $CDCl_3$, only 5% of product **4** was detected after 16 h at 50 °C (Table 1, entry 12). In the presence of $B(Ph)_4^-$ as counteranion (**5e**) (Table 1, entry 14) the product **4** was isolated in 50% yield, a value significantly lower than that obtained in the presence of iodide as counteranion (98%).

These data clearly indicate that the catalytic efficiency of the *p*-iodophenyltrimethylammonium co-catalyst is strongly affected by the counteranion. The two salts **5a** and **5d** show different solubility in the reaction medium, in fact, when the *p*-iodophenyltrimethylammonium **5a** was mixed with **2** and **3**, in the presence of **1** in water-saturated $CDCl_3$, then a homogenous solution was obtained, while the analogous experiment in the presence of 5**d** (BF_4^- salt of *p*-iodophenyltrimethylammonium) led to the formation of a suspension of the salt. Besides, data previously reported by Rebek,[17] highlighted that the tetraalkylammonium salts of I^- and BF_4^- both form a resorcinarene aggregate but the ^{1}H NMR spectra of the two complexes differ starkly. In accord with this, DOSY studies reported by Cohen[18] showed that the tetraethylammonium iodide and tetraethylammonium BF_4^- are encapsulated inside resorcinarene aggregate that haven't the same structure for the two different anions. These results suggest that probably after the encapsulation of **5d** a resorcinarene aggregate was formed, which was catalytically inactive.

In Silico Studies

In order to study the role of the halogen-bonding interaction in the activation of **3**, we conducted a quantum chemical investigation. To this purpose, we chose, as a representative model, the reaction between **2** and **3**, using a reduced capsule (**C_{R6}**) with methyl feet and ONIOM method (M06-2X:PM6).[13,15,19] The stabilization energy of the complexes calculated by QM method suggests that the first species to enter in the capsule is **5a** followed by **3** and then by **2** (Table S1, entries 1, 5, 8).

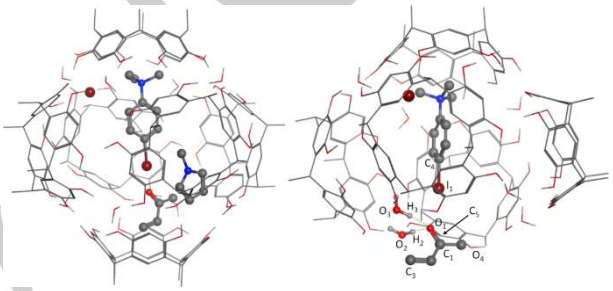

Figure 2. Full optimized geometries of [**5a+2+3**]@**C_{R6}** (left), and [**5a+3**]@**C_{R5}** (right) complexes. The arbitrary numbers on the selected atoms were introduced to understand the subsequent analysis employing the second-order perturbation theory (SOPT).[20]

In addition, the results (SI) clearly indicates that the counteranion I^- prefers to stay inside the capsule, stabilized by hydrogen bond interactions with a bridging water molecule. QM-calculations indicate that the halogen-bonding interaction between **5a** and **3** inside **C_6** forces the reagents along the axis that joins two vertexes of the octahedral capsule (Figure 2, left). In this way, they are able to engage a halogen bond, but the pyrrole **2** is sterically unable to interact with the β-carbon of **3**, and we were not able to locate any effective TS geometry for the studied Michael addition without the loss of the halogen bond interaction. Due to this mandatory requirement for the geometry of the reactants, we supposed to work with a reduced pentameric capsule (Figure 2 right, **C_{R5}**) in which a resorcinarene unit is removed.[21] Interestingly, a recent report by Schalley and coworkers showed the existence of a pentameric cluster of resorcin[6]arene units by HR FT ICR mass spectrometry.[22] In this way, we were able to find a stationary geometry in which not only the reactants **5a** and **3** are able to engage a halogen bond that is preserved during the Michael addition, but the carbonyl oxygen of **3** is also able to establish two supplementary hydrogen bonds with two bridging water molecules of the pentameric resorcinarene structure (Figure 2, right); this last event ulterior activate the reaction, synergistically enhancing the halogen bond effect. In this geometry, three methyl groups of **5a** are symmetrically pointing inside the π-electron-rich cavity of a resorcinarene macrocycle, and the reagents are located in the same axis that joins two vertexes of the original octahedral geometry of the capsule, but the methyl vinyl ketone **3** is pointing outside the cavity of the capsule. Even in this case, the

10.1002/anie.201909865

counteranion establishes hydrogen bond interactions with a bridging water molecule. The calculated energies suggested an enthalpic and a free Gibbs energy stabilization for the reactants **2**, **3**, and **5a** after the complexation.

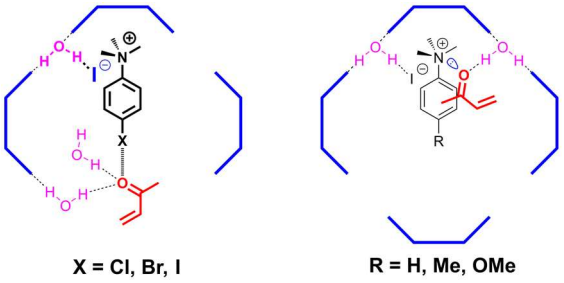

Figure 3. Schematic representation of the two alternative mechanistic routes proposed for the supramolecular catalyzed Michael addition.

Subsequently, obtained the correct geometry with the pyrrole conveniently placed to carry out the Michael addition, the effect of three different halogens (iodine, bromine, and chlorine) was evaluated by measuring the activation energies attributable to the transition states for the reaction inside the capsule, considering the halogen bond donors **5a**–**c** and the reactants **2** and **3**. The free Gibbs activation energy involved in the first step of the addition of the *N*-methylpyrrole **2** to the α,β-unsaturated enone **3** justify the trend of experimentally observed yields (Table S1, entries 12–14). Although this result seems to go against the classical trend linked to the strength of the halogen bond (I > Br > Cl), we will see that it is not so (see the discussion on the SOPT analysis). Moreover, we studied the Michael reaction between **2** and **3** in the presence of **5a** but in the absence of halogen-bonding interactions between **5a** and **3**. Differently from the geometry in Figure 3 (left), when the carbonyl group of **3** did not establish halogen-bonding interactions with **5a**, then a hydrogen bonding interaction was found with a bridging water molecule (Figure 3, right). Significantly, in this geometry (Figure 3, right) the carbonyl group of **3** was located close to the positively charged nitrogen of **5a**. The pyrrole **2** was located in a position able to interact with the β-carbon of **3**. The activation energy for this reaction resulted in 26.44 kcal/mol (Table S1, entry 9), which is 6.28 kcal/mol higher than that of the reaction catalyzed through halogen bonding, suggesting again that the effects of the halogen interaction can lower the energy barrier. Finally, the calculated activation energy for the reaction in the absence of the catalyst resulted in 28.28 kcal/mol (Table S1, entry 15), confirming the pivotal role of the capsule in this reaction. Thus, these results are entirely in accordance with the experimental ones; in fact, when **2** and **3** were reacted in the presence of **1**, under the conditions reported in Scheme 1 and Table 1, in the presence of phenyltrimethylammonium **5h** (Table 1, entry 18) then 33% of **4** was obtained, according to the calculated activation free energy of 27.06 kcal/mol (Table S1, entry 17). Analogously, lower yields of **4** were obtained in the presence of **5f** (*p*-Me, Table 1 entry 16) and **5g** (*p*-MeO, Table 1 entry 17) confirming the crucial role played by the halogen atom in the *para*-position of **5** for the Michael reaction reported in Scheme 1.

Furthermore, to assess the solvent effect on the most crucial rate-determining step of this reaction, the activation energies for the investigated TSs were further calculated in chloroform (Table S1). The results are substantially in line with those obtained in the gas phase; substantially, there was only an increase in the free activation energies in the range 1.71–3.34 kcal/mol.

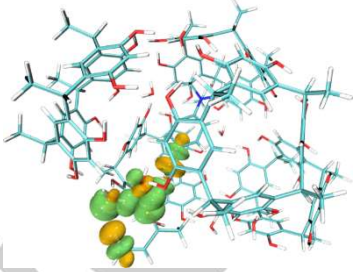

Figure 4. Selected principal orbital interactions for [**5a+3**]@$\mathbf{C_{R5}}$ as derived by the SOPT analysis.

To further validate and elucidate the obtained results on the reactivity of this system, especially on the contributions due by H-bond, halogen-bond, and other non-covalent interactions (NCI), we indagate on the geometries of selected stationary points with some of the powerful tools of the conceptual density functional theory. For this purpose, we have selected the local electrophilicity (ω_k), according to the recently improved definition of Domingo),[23] the interaction energies [$E^{(2)}$] arising from the SOPT analysis of the Fock matrix in NBO basis, according to the definition of delocalization energy given by Weinhold,[20] and the non-covalent interactions (NCI) index proposed by Yang's group. Interestingly, the SOPT analysis (Figure 4) conducted on the [**5a+3**]@$\mathbf{C_{R5}}$, [**5b+3**]@$\mathbf{C_{R5}}$, and [**5c+3**]@$\mathbf{C_{R5}}$ complexes (Table S2) indicates that they are stabilized, also, by a dense network of H-bond and halogen-bond interactions.

In particular, for the investigated complexes, we calculated the $n\rightarrow\sigma^*$ interaction between the carbonyl O_1 (n) and the antibonding orbitals (σ^*) of the O_2–H_2 and O_3–H_3 (Figure 4, refer to Figure 2 for the numeration) single bonds of the two water molecules. These interactions account for total energy of 14.13, 13.13, and 14.26 kcal/mol for [**5a+3**]@$\mathbf{C_{R5}}$, [**5b+3**]@$\mathbf{C_{R5}}$, and [**5c+3**]@$\mathbf{C_{R5}}$ complexes, respectively (Table S2, entries 4–6).

Moreover, the $n\rightarrow\sigma^*$ interactions of the carbonyl O_1 lone pairs with the antibonding orbital of the C_4–X_1 single bond, that highlight the formation of an halogen bond, have a value of 1.70, 1.66, and 1.33 kcal/mol for the iodine, bromine, and chlorine-containing complexes, respectively (Table S2, entries 8,9, and Figure 4 for iodine), that is in accord with the classical trend linked to the strength of the halogen bond. Based on these and others[24] (Table S2, entries 1–3, 7, and 10–12) energy analyses (Table S2), emerges that the stability order for the complexes at hand is [**5a+3**]@$\mathbf{C_{R5}}$ > [**5c+3**]@$\mathbf{C_{R5}}$ > [**5b+3**]@$\mathbf{C_{R5}}$ (21.30 > 19.85 > 19.78 kcal/mol, Table S2, total energy) due to a complex synergistic balance between H-bonds, halogen-bond, and non-covalent interactions (see Supporting Information, #9.2 and Figure S54).

Since the electron density transfer taking place in the transition states [**5a+2+3**]@$\mathbf{C_{R5}}$-TS, [**5b+2+3**]@$\mathbf{C_{R5}}$-TS, and [**5c+2+3**]@$\mathbf{C_{R5}}$-TS, in terms of the residual charge of *N*-

methylpyrrole **2** fragment, is high (0.428, 0.431, and 0.437 au, respectively) the process can be considered polar and the reactivity directly correlated to the local electrophilicity of the C_3 β-carbon atom of the reagent **3** (ω_{C_3}). The values obtained for the ω_{C_3} (Table S3) are consistent with the efficiency of the above described catalytic ensemble exerted on the generation of a most potent electrophilic C_3 center; in fact, the highest value of ω_{C_3} has been registered for the [**5a**+**3**]@$\mathbf{C_{R5}}$ complex followed by the [**5a**+**3**]@$\mathbf{C_{R6}}$, [**5c**+**3**]@$\mathbf{C_{R5}}$, [**5b**+**3**]@$\mathbf{C_{R5}}$, and [**5a**+**3**] ones (Table S3, entries 1,4,3,2, and 5, respectively), according to the experimental results. In particular, it is evident that the competition between the halogen bond activated pentameric complex and the non-halogen bond activated hexameric complex is in favor of the former (Table S3, entry 1 *vs*. entry 4). Finally, the halogen bond activated complex without the presence of the capsule shows the smallest ω_{C_3} value (Table S3, entry 5), whose magnitude is not sufficient to support an efficient nucleophilic attack.

Thus, the SOPT analysis and, mostly, the electrophilic indices account for the striking higher activity of the XB catalyst **5c** with respect to **5b**. In fact, even if Br is an XB donor group more strong than the Cl one, the XB catalyst **5c** is moderately more active than **5b**, because the former shows a higher local electrophilicity value (Table S3, entries 2 and 3). Moreover, from the examination of Table S3, comparing the entries 1 and 5, it can be deduced that the halogen bond, for iodine, affects approximately 50% on the value of electrophilicity; the remaining is attributable to all the other interactions. Therefore, presumably, the halogen bond that involves iodine affects 50% of the activation of the reaction studied here.

The tentative to computationally rationalize the observed effects for the different studied counterions failed; however, this is in accord with other studied reactions which involve the halogen bond catalysis: the effects vary both with the type of reaction and with the type of solvent used, and it is not predictable. [25]

High-Resolution FT-ICR ESI-MS and DOSY Studies

Experimental evidences of the presence of a pentameric resorcinarene capsule $\mathbf{C_5}$ under the catalytic reaction conditions were collected by DOSY studies and HR FT-ICR ESI MS (Figures 5 and 6). As reported in Figures 5a,b when the reactants **2** and **3** were added to a solution of the complex **5a**@$\mathbf{C_6}$ then a strong increasing of the diffusion coefficient of the capsule was observed (from –10.57 to –9.70 m^2/sec, Figure 5a (I and II) and Figure 5b) in accord with the variation of the molecular size of the supramolecular complex in solution. Of course, this is compatible with the loss of a resorcinarene unit (**5a**@$\mathbf{C_6}$ − 1105.7 Da). Very significantly, the diffusion coefficient remains practically constant during the reaction progress (Figure 5b,c), while it returns to the initial value (about −10.35 m^2/sec, see Figure 5a,b) after 14 h, when the conversion of the reactants to product **4** was 95% (Figure 5c), and no reactants were left over to form the pentameric capsule. At this point, the hexameric complex **5a**@$\mathbf{C_6}$ was formed back again.

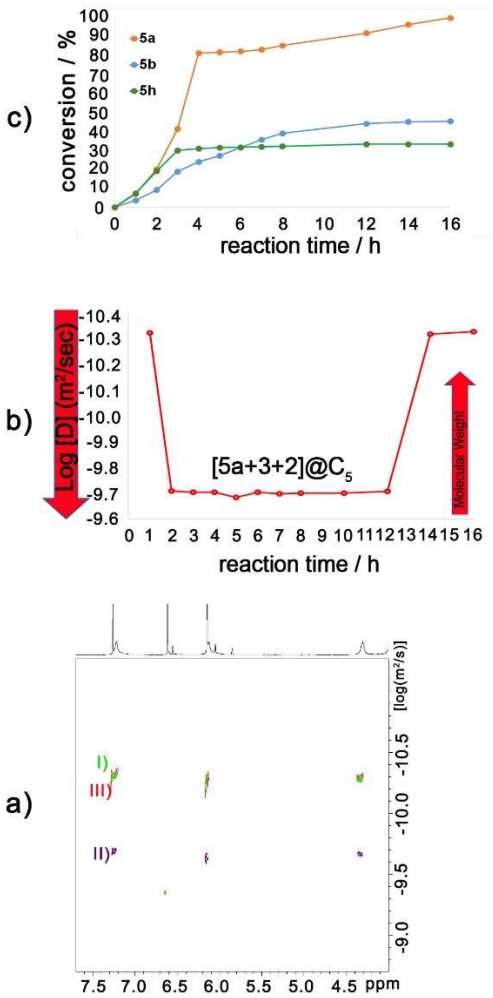

Figure 5. a) Overlapped DOSY spectra of the mixture of **1**, **2**, **3** and **5a** in water-saturated $CDCl_3$ (600 MHz, 298 K), after: I) 1h, II) 5h and III) 14h. b) Diffusion coefficients of the resorcinarene capsule measured during the reaction between **2** and **3** in the presence of **5a**; c) The conversion of the reaction in Scheme 1 in the presence of different catalysts.

Kinetic studies (Figure 5c) were performed for the reaction in Scheme 1 using the catalyst **5a**, **5b** and the non-halogenated catalyst **5h,** used as reference compounds. We aimed to assess the efficiency of the two alternative mechanistic routes proposed in Figure 3 for the halogenated and non-halogenated catalysts in Scheme 1. In fact, using catalyst **5h** the catalytic mechanism in Figure 3 (left) should be operative in which an H-bond, with a bridging water molecule, and ion-dipole interactions should be accountable for the activation of the substrate **3**. In the presence of derivatives **5a**,**b**, the H-bonding interaction should be again catalytically active, but also the halogen-bonding interaction with the catalyst should be established (Figure 3 left). In this way, by comparing the catalytic performance of **5a** and **5h** we could evaluate the role of the halogen-bonding interactions in the catalysis of the reaction in Scheme 1. In the presence of non-halogenated catalyst **5h** we observed a slight activity (Figure 6c, green line), in the initial part of the reaction, which does not evolve in the complete transformation of reagents into the products;

10.1002/anie.201909865

probably, the observed reactivity is due to the mechanistic route in Figure 3 (right).

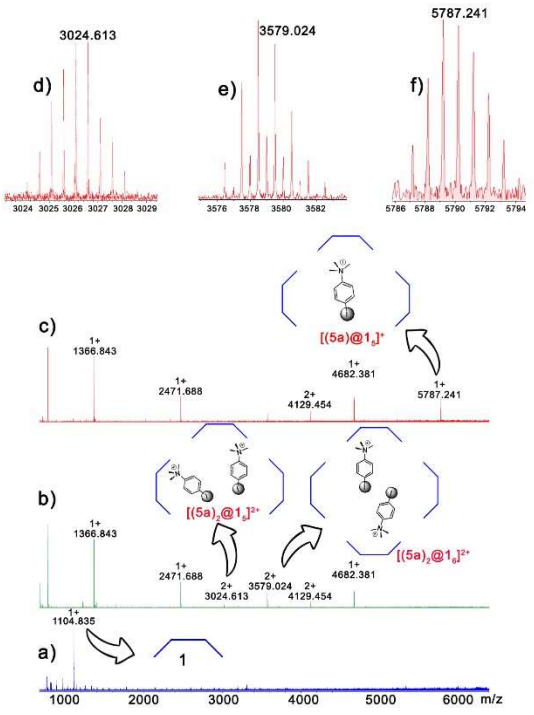

Figure 6. ESI - FTICR mass spectra of: a) a 250 μM solution of **1** in water-saturated $CHCl_3$, b) after addition of stoichiometric amounts of **5a**, c) mixture in (b) in the presence of **2** and **3** (same reaction conditions), Experimental patterns of d) $[(\mathbf{5a})_2@\mathbf{1_5}]^{2+}$, e) $[(\mathbf{5a})_2@\mathbf{1_6}]^{2+}$, and f) $[\mathbf{5a}@\mathbf{1_5}]^{2+}$.

The kinetic profile in the presence of catalysts **5a**,**b** shows different reaction courses. In detail, bromine-based catalyst **5b** led to a conversion of 45% after 16 hours (Figure 5c, blue line). Regarding catalyst **5a**, the kinetic profile of the reaction (Figure 5c, orange line) shows a sigmoidal shape (analogously for **5h**) in which an initial lag-phase (for the first 2 h) is followed by a strong increase in the reaction rate. Thus, an 80% conversion in product was observed after 4 h, while during the remaining 12 h another 18% of conversion was collected. Probably, the formation of a stable, catalytically less active complex (e.g.: **5a+2@C$_5$** or **4@C$_5$**) could be envisioned in order to explain the plateau observed after 4h in the kinetic profile of **5a** (Figure 5c, orange line). In conclusion, in accord with the QM calculations, the halogen bonding interaction plays a pivotal role in the activation of the carbonyl group of **3.**

As concerns the presence of the pentameric capsule, useful insights in this aspect have been obtained by HR-FTICR-ESI mass spectrometry (Figure 6). When resorcinarene **1** was ionized with an ESI source in the absence of catalyst **5a**, then only the molecular peak of **1** at 1104.835 *m/z* was detected (Figure 6a). Differently, when an equimolar mixture of resorcinarene **1** and catalyst **5a** was ionized with an ESI source according to the conditions reported previously by Schalley and coworkers[22] then the mass spectrum reported in Figure 6b was obtained. The results in Figure 6b suggested that the organic cation of **5a** templates the formation of pentameric $(\mathbf{5a})_2@\mathbf{1_5}$ and hexameric $(\mathbf{5a})_2@\mathbf{1_6}$ aggregate, which were detected at 3024.613 *m/z* and 3579.024 *m/z,* and in which two units of **5a** were present inside the capsules. Significantly, when the reactants **2** and **3** were added to the mixture in Figure 6b then the mass spectrum in Figure 6c was obtained, in which a peak at 5787.24 *m/z* was revealed attributable to the pentameric aggregate containing a single unit of catalyst **5a**, $(\mathbf{5a}@\mathbf{1_5})$**.** Under these conditions no hexameric capsule was detected. In conclusion, MS studies confirm the presence of a pentameric capsule, in addition they provide an useful suggestion to explain the initial lag-phase in the kinetic profile of **5a** (and **5h**). Probably, because of the greater affinity of the cationic guests for the resorcinarene capsule, after the initial addition of **5a** a complex $(\mathbf{5a})_2@\mathbf{C_6}$ was formed (Scheme 2) in which two units of **5a** were included into the cavity of the hexameric capsule. Consequently, time was required for the formation of the heterocomplex **[5a+3+2]@C$_5$**.

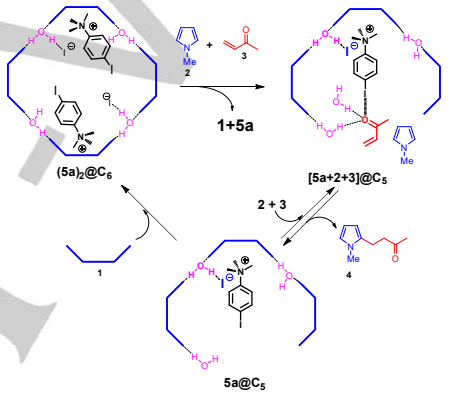

Scheme 2. Proposed mechanism for the Michael reaction in Scheme 1 through the formation of the pentameric capsule **C$_5$** as extrapolated by QM calculations, DOSY, and HR FTICR ESI MS studies in Figure 6.

Conclusion

In conclusion, by analyzing both the experimental and *in-silico* results, we can conclude that the studied Michael reaction can occur in a nanoconfined space through the activation of the electrophile **3** by XB interactions with the *p*-iodophenyltrimethyl-ammonium co-catalyst, with the additional assistance of HB interactions with the bridging water molecules. Quantum-mechanical calculations strongly corroborated the presence of an XB interaction between **5a**–**c** and **3** in the nanoconfined space of an open pentameric capsule. Here, the XB co-catalyst **5a** is kept inside through cation···π interactions with the *π*-electron-rich cavity. Finally, evidences or the formation of a pentameric resorcinarene capsule were obtained by DOSY studies and HR FTICR ESI mass spectra.

Halogen Bonding • Catalysis • Nanoconfined • Resorcinarene Capsule

[1] [1] G. Cavallo, P. Metrangolo, R. Milani, T. Pilati, A. Priimagi, G. Resnati, G. Terraneo, *Chem. Rev.* **2016**, *116*, 2478-2601. P. Metrangolo, G. Resnati, *Halogen Bonding- Fundamentals and Applications*, Springer-Verlag, Berlin, **2008**.

[2] L. C. Gilday, S. W. Robinson, T. A. Barendt, M. J. Langton, B. R. Mullaney, P. D. Beer, *Chem. Rev*. **2015**, *115*, 7118-7195.

[3] a) A. Priimagi, G. Cavallo, P. Metrangolo, G. Resnati, *Acc. Chem. Res.* **2013**, *46*, 2686–2695. b) H. Takezawa, T. Murase, G. Resnati, P. Metrangolo, M. Fujita, *Angew. Chem. Int. Ed. Engl.* **2015**, *54*, 8411 – 8414. c) M. G. Sarwar, D. Ajami, G. Theodorakopoulos, I. D. Petsalakis, J. Rebek, Jr. *J. Am. Chem. Soc.* **2013**, *135*, 13672–13675.

[4] a) T. Clark, M. Hennemann, J. S. Murray, P. Politzer, *J. Mol. Model.* **2007**, *13*, 291–296. B) P. Politzer, J. S. Murray, T. Clark, *Phys. Chem. Chem. Phys.* **2010**, *12*, 7748–7757

[5] a) S. Benz, A. I. Poblador,-Bahamonde, N. Low-Ders, S. Matile *Angew. Chem. Int. Ed*. **2018**, *57*, 5408-5412. b) R. Tepper, U. S. Schubert *Angew. Chem. Int. Ed*. **2018**, *57*, 6004-6016, and reference cited therein.

[6] a) D. Bulfield, S. M. Huber *Chem. Eur. J.* **2016**, *22*, 14434–14450, and reference cited therein. B) A. Bruckmann, M. A. Pena, C. Bolm, *Synlett* **2008**, 900-902.

[7] J.-P. Gliese, S. H. Jungbauer, S. M. Huber, *Chem. Commun*. **2017**, *53*, 12052-12055.

[8] a) S. M. Walter, F. Kniep, E. Herdtweck, S. M. Huber, *Angew. Chem. Int. Ed*. **2011**, *50*, 7187-7191. b) F. Kniep, S. H. Jungbauer, Q. Zhang, S. M. Walter, S. Schindler, I. Schnapperelle, E. Herdtweck, S. M. Huber, *Angew. Chem. Int. Ed*. **2013**, *52*, 7028-7032.

[9] F. Heinen, E. Engelage, A. Dreger, R. Weiss, S. M. Huber, *Angew. Chem. Int. Ed*. **2018**, *57*, 3830-3833.

[10] a) Ajami, D.; Rebek, J. Jr. *Acc. Chem Res.* **2013**, *46*, 990–999. b) Rebek, J. Jr. *Acc. Chem Res.* **1999** *32*, 278–286. c) L. Catti, Q. Zhang, K. Tiefenbacher, *Chem. Eur. J.* **2016**, *22*, 9060−9066. d) Rebek, Jr. J. *Angew. Chem. Int. Ed. Engl.* **2005**, *44*, 2068 – 2078. e) G. Borsato, J. Rebek, Jr., A. Scarso, in *From Selective Nanocatalysts and Nanoscience* (Eds.: A. Zecchina, S. Bordiga, E. E. Groppo), Wiley-VCH Verlag GmbH & Co. KGaA, Weinheim, Germany, **2011**, pp. 105-168. f) L. Avram, Y. Cohen, J. Rebek, Jr. *Chem. Commun.* **2011**, *47*, 5368−5375. g) G. Borsato, A. Scarso, *in Organic Nanoreactors* (Ed.: S. Sadjadi), Academic Press, **2016**, Chapt. 7, pp. 203−234. h) L. Catti, T. Brauer, Z. Qi, K. Tiefenbacher, *Chimia*, **2016**, *70*, 810−814. i) S. S. Nurttila, P. R. Linnebank, T. Krachko, J. N. H. Reek, *ACS Catal.* **2018**, *8*, 3469–3488. j) S. H. A. M. Leenders, R. Gramage-Doria, B. de Bruin, J. N. H. Reek, *Chem. Soc. Rev.* **2015**, *44*, 433-448. k) M. Yoshizawa, J. K. Klosterman, M. Fujita, *Angew. Chem. Int. Ed.* **2009**, *48,* 3418 – 3438. l) Q. Zhang, L. Catti, K. Tiefenbacher, *Acc. Chem. Res.* **2018**, *51*, 2107−2114. m) C. Gaeta, C. Talotta, M. De Rosa, P. La Manna, A. Soriente, P. Neri, *Chem. Eur. J*. **2019**, *25*, 4899–4913.

[11] a) D. J. Cram, *Nature* **1992**, *356*, 29–36. b) D. J. Cram, J. M. Cram, *Container Molecules and Their Guests,* The Royal Society of Chemistry, Cambridge, U.K. 131–216, 1994.

[12] M. M. Conn, J. Rebek, *Chem. Rev*. **1997**, *97*, 1647-1668.

[13] P. La Manna, C. Talotta, G. Floresta, M. De Rosa, A. Soriente, A. Rescifina, C. Gaeta, P. Neri, *Angew. Chem. Int. Ed*. **2018**, *57*, 5423–5428.

[14] a) L. R. MacGillivray, J. L. Atwood, *Nature* **1997**, *389*, 469-472; b) A. Shivanyuk, J. Rebek, *J. Am. Chem. Soc*. **2003**, *125*, 3432-3433; c) L. Avram, Y. Cohen, *Org. Lett*. **2002**, *4*, 4365-4368. d)

[15] P. La Manna, M. De Rosa, C. Talotta, C. Gaeta, A. Soriente, G. Floresta, A. Rescifina, P. Neri, *Org. Chem. Front*. **2018**, *5*, 827-837.

[16] T. M. Bräuer, Q. Zhang, K. Tiefenbacher, *Angew. Chem. Int. Ed*. **2016**, *55*, 7698-7701.

[17] A. Shivanyuk, J. Rebek Jr. *Proc. Natl. Acad. Sci. USA 94*, **2001**, *98*, 7662–7665.

[18] L. Avram, Y. Cohen *Org. Lett.* **2008**, *10*, 1505–1508.

[19] S. Gambaro, M. De Rosa, A. Soriente, C. Talotta, G. Floresta, A. Rescifina, C. Gaeta, P. Neri, *Org. Chem. Front*. **2019**, *6***,** 2339–2347**.**

[20] F. Weinhold, C. R. Landis, *Valency and bonding: a natural bond orbital donor-acceptor perspective*, Cambridge University Press, Cambridge, UK; New York, **2005.**

[21] A tentative to work with an exotic semi-open “packman like” capsule failed due to the take-over of hydrogen bonds network between the two bridging water molecules and the phenol hydroxyls.

[22] N. K. Beyeh, M. Kogej, A. Ahman, K. Rissanen, C. A. Schalley, , *Angew. Chem. Int. Ed*. **2006**, *45*, 5214–5218.

[23] L. R. Domingo, P. Perez, J. A. Saez, *RSC Adv*. **2013**, *3*, 1486-1494.

[24] Another important stabilization of almost equal entity (1.9 kcal/mol) is established between the O_2 of a bridging water molecule of $\mathbf{C_{R5}}$ (see Figure 3, right and Figure 4) with the antibonding orbital of the C_3–H_4 single bond of **3** (Table S2, entry 12).

[25] a) S. M. Walter, F. Kniep, E. Herdtweck, S. M. Huber, *Angewandte Chemie-International Edition* **2011**, *50*, 7187-7191; b) S. H. Jungbauer, S. M. Walter, S. Schindler, L. Rout, F. Kniep, S. M. Huber, *Chem. Commun*. **2014**, *50*, 6281-6284; c) S. H. Jungbauer, S. M. Huber, *J. Am. Chem. Soc*. **2015**, *137*, 12110-12120; d) D. von der Heiden, E. Detmar, R. Kuchta, M. Breugst, *Synlett* **2018**, *29*, 1307-1313

Acknowledgements

The authors acknowledge the Regione Campania (POR CAMPANIA FESR 2007/2013 O.O.2.1, CUP B46D14002660009) for the FT-ICR mass spectrometer facilities, Farma-BioNet (CUP B25C13000230007), the Centro di Tecnologie Integrate per la Salute” (CITIS) (project PONa3_00138), for the 600 MHz NMR facilities. Financial support is acknowledged from the Università di Salerno (FARB 2017 “Composti Macrociclici come Organocatalizzatori Supramolecolari in Catalisi Biomimetica”).

Keywords: Halogen Bonding • Catalysis • Nanoconfined • Resorcinarene Capsule

10.1002/anie.201909865

WILEY-VCH

RESEARCH ARTICLE

Closer and stronger. *The amplification of the halogen bonding in a small space introduced by Rebek in 2013 is here exploited for the activation of the methyl vinyl ketone in a Michael reaction. The reaction occurs in the nano-confined space of a recorcinarene capsule where the XB catalyst is effective. No reaction occurs in the bulk medium in absence of capsule.*

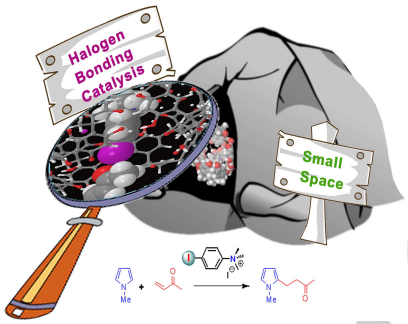

Pellegrino La Manna, Margherita De Rosa, Carmen Talotta, Antonio Rescifina,* Giuseppe Floresta, Annunziata Soriente, Carmine Gaeta,* and Placido Neri*

Page No. – Page No.

Synergic Interplay Between Halogen Bond and Hydrogen Bond in the Activation of a Neutral Substrate in a Nanoconfined Space